J. Fluid Mech. (1990), *vol.* 216, *pp.* 629–656
Printed in Great Britain

Flow over a leading edge with distributed roughness

By J. M. FLORYAN[1] AND U. DALLMANN[2]

[1] Department of Mechanical Engineering, The University of Western Ontario, London, Ontario N6A 5B9, Canada

[2] Institute for Theoretical Fluid Mechanics, German Aerospace Research Establishment, D-3400 Göttingen, FRG

(Received 11 October 1988 and in revised form 9 January 1990)

An analysis of the flow over a leading edge with distributed roughness is presented. The analysis is focused on a small neighbourhood of the stagnation line. The roughness is assumed to have a small amplitude and to be symmetric with respect to the stagnation line. Results show that roughness acts as a source of streamwise vorticity. The existence of a universal form of the flow field for long-wavelength roughness is demonstrated. It is shown that surface stresses tend to eliminate roughness if erosion or wall flexibility are admitted. The heat flow tends to concentrate at the tips of the roughness and this may lead to the generation of large thermal stresses along the surface of the leading edge.

1. Introduction

The understanding of the laminar–turbulent transition process in boundary layers is still one of the open questions in fluid mechanics, mainly because of the large number of possibly important factors present. While a tremendous amount of work has been devoted to the analysis of stability of boundary layers, relatively little effort has been spent on understanding mechanisms governing the so-called receptivity problem, i.e. mechanisms by which disturbances enter the boundary layer (Reshotko 1976). Goldstein (1983) was the first to demonstrate a process through which free-stream disturbances can enter the boundary layer around the leading edge; however, the stagnation flow region was excluded from consideration. The analysis of flow close to a stagnation line is of primary importance since this is where the boundary layer originates and where the disturbances could first penetrate into it. The leading-edge boundary layer is characterized by a high divergence, i.e. velocity components normal and tangential to the wall are of the same order, and by a very small thickness. The second factor makes it very susceptible to the presence of surface roughness. Obviously, if the leading-edge flow cannot be kept laminar and stable, it is unlikely that the boundary layer further downstream can be kept laminar. This has been vividly demonstrated in the case of the so-called 'attachment line (or leading edge) contamination' (Pfenninger 1977; Poll 1979).

It has been shown that large surface roughness at the leading edge could trip the boundary layer and lead to a turbulent flow over a whole body (Poll 1979). Small surface roughness modifies the boundary layer and makes it more susceptible to different types of instability. Surface roughness can, for example, generate spanwise periodicity of the flow and this, in turn, could accelerate the growth of Tollmien–Schlichting waves further downstream. Interaction mechanisms between

travelling waves and stationary spanwise periodic structures have been shown to lead to a rapid growth of Tollmien–Schlichting waves (Nayfeh 1981; Srivastava & Dallmann 1987) as well as Görtler vortices (Floryan & Saric 1984). In the case of a three-dimensional boundary layer, roughness-generated spanwise periodicity could affect cross-flow instabilities through an interaction mechanism of the type studied by Fischer & Dallmann (1987). The existence of coupling between very small leading-edge imperfections and the disturbance structure further downstream has been confirmed by recent experiments on the stability of three-dimensional boundary layers (Nitschke-Kowsky & Bippes 1988; Nitschke-Kowsky 1986). It has been found that the disturbance structure is fixed with respect to the plate when the plate was moved in the spanwise direction in the wind tunnel, and this coupling could not be eliminated by polishing of the leading edge using standard methods (H. Bippes 1988, private communication).

Stagnation flow at the leading edge is subject to its own peculiar instability which manifests itself by the appearance of counter-rotating vortex pairs with their axes parallel to the streamwise direction (see Morkovin 1979 for a review). It has been suggested by Görtler (1955) that the secondary flow results from the action of centrifugal forces. Wilson & Gladwell (1978) have shown that the flow is linearly stable, if the disturbances originate from within the boundary layer. Lyell & Huerre (1985) have suggested that the flow can be destabilized through nonlinear mode coupling if the level of these disturbances is sufficiently high, but Spalart (1989) was unable to find such nonlinear effects in his numerical experiments and suggested that results of Lyell & Huerre (1985) were artifacts of their method of solution. Sutera, Meader & Kestin (1963) and Sutera (1965) have put forward an alternative theory, which requires the presence in the oncoming stream of a certain type of disturbance, which is amplified by the so-called 'vorticity amplification mechanism' while being swept towards the body. In a recent experiment, Kottke (1986) and Böttcher (1987) were able to find vortices only if disturbances produced by screens were present upstream of the body. The spacing of the vortex pairs was found to be equal to that of the jets in the wake of the screen. Thus, the flow in the stagnation region was merely an image of the flow downstream of the screens and no indication of the existence of a stagnation-point instability was found. Surface roughness could be an alternative source of disturbances and could lead to the appearance of vortices either through the vorticity amplification mechanism or through some type of interaction, even if the oncoming flow is free of disturbances. Thus, surface roughness can modify stagnation flow directly, by forcing it to conform to the geometry of the surface, and indirectly, by providing a disturbance environment necessary to trigger an instability mechanism leading to the appearance of the secondary flow.

It is known that disturbances present in the oncoming stream have a very strong effect on heat transfer in the stagnation region with very little change in skin friction (Kestin 1966). While the vorticity amplification mechanism explains qualitatively certain observed features (Sutera *et al.* 1963; Sutera 1965), it fails to explain the observed phenomena completely (Kestin 1966). It is also known that surface roughness enhances heat transfer (Morgan 1973); however, the mechanics of the process is not clear. It is not certain how strong this effect is in the stagnation region, since no detailed measurements dealing with this particular flow area are available. It remains to postulate that the changes in the heat transfer in the stagnation region could occur because of additional mixing caused by the irregularities of the surface or, perhaps, by a secondary flow which is triggered by the disturbance environment resulting from the presence of the surface roughness.

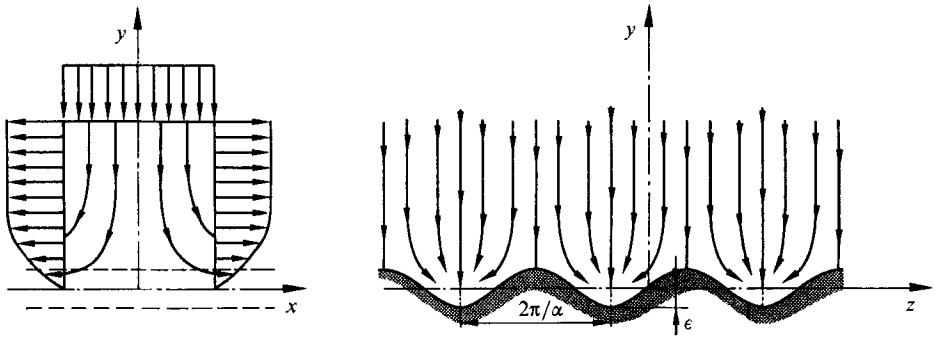

FIGURE 1. Schematic diagram of a stagnation flow over a plate with a wavy surface roughness.

The purpose of this paper is to analyse modifications of the stagnation flow caused by the presence of a small distributed surface roughness. The resulting non-uniform flow might be subject to an instability mechanism which is different from the classical one studied previously (Wilson & Gladwell 1978). The results provide initial conditions necessary for tracking effects of surface roughness further downstream. Further applications include the determination of the increase of heat transfer due to the presence of roughness, and the determination of shear and normal stress increases with applications to erosion and ablation. Section 2 describes the formulation of the governing equations. Section 3 summarizes results dealing with the stagnation flow over a smooth plate needed for further analysis. Section 4 discusses disturbance equations and methods used for determination of their solutions. Section 5 provides discussion of the effects associated with the presence of surface roughness.

2. Problem formulation

We consider a steady, incompressible, constant-properties flow over an infinite plate with a distributed roughness on its surface. The plate is oriented normal to the direction of an initially uniform stream. The geometry of the flow and the coordinate system are indicated in figure 1. The plate is essentially in the (x, z)-plane and the basic flow in the absence of roughness is two-dimensional in the (x, y)-plane, the x-axis being the streamwise direction along the plate, and the z-axis the spanwise direction. The stagnation streamline coincides with the y-axis. The configuration described above provides a good approximation of a flow in the neighbourhood of the forward stagnation point on cylindrical bodies with axis normal to the direction of the oncoming stream (Morkovin 1979).

We consider the amplitude of the roughness to be small compared with the boundary-layer thickness. The roughness produces a three-dimensional modification of the flow field which, in the limit of small roughness amplitude, is described by linear equations. We consider the roughness to be distributed, i.e. its variations are representable by means of a Fourier decomposition. We limit our considerations to a small neighbourhood of the stagnation line and roughnesses that are symmetric with respect to the (y, z)-plane. Since variations of the shape of the roughness can also be represented as power series in terms of distance from the stagnation line, the roughness becomes independent of x close to the stagnation line. It is then sufficient to consider the flow over a wall described by an equation (see figure 1)

$$y = \epsilon \sin(\alpha z), \tag{2.1}$$

while the flow over a roughness having an arbitrary amplitude distribution in the spanwise direction can be represented by a Fourier superposition of such 'modal' flows.

The model problem considered above is fairly general and the results can be used to describe flows over symmetric but otherwise arbitrary rough leading edges. The validity of the results is restricted to a small neighbourhood of the stagnation line. The effects of variations of the form of the roughness in the streamwise direction can be accounted for by considering the full expansions in terms of distance away from the stagnation line. Such a procedure would be similar to the Blasius series expansions in boundary-layer theory. As stated before, the solution presented here is limited only to the first term of such an expansion. While the analysis of the roughness effects is the main motivation for our work, the model problem described above also corresponds to a flow over an infinite flat plate with riblets of fixed shape extending to $\pm\infty$ in the streamwise direction, i.e. the flow over an infinite flat plate with riblets and flow over a rough leading edge are identical close to the stagnation line.

We select the boundary-layer thickness δ as a lengthscale and the upstream velocity V_∞ as a velocity scale. Here, $\delta = (\nu/K)^{\frac{1}{2}}$ where ν stands for kinematic viscosity and K is defined by the character of the velocity field away from the plate, i.e. $u^* \to Kx^*$ as $y^* \to \infty$. Asterisks denote dimensional quantities and u is the velocity component in the x-direction. We define the dimensionless temperature as $T = (T^* - T_\infty)/T_s$, where T_∞ stands for the temperature of the oncoming stream and T_s is the temperature scale. Here $T_s = T_w - T_\infty$ in the case of an isothermal plate and $T_s = h\delta$ in the case of a constant heat flux across the plate. T_w is the plate temperature and h denotes the dimensional temperature gradient at the wall. We also rescale the dimensionless x-coordinate, i.e. we let $X = x/Re$, Re being the Reynolds number based on V_∞ and δ.

We assume that each flow quantity is the sum of two parts, a mean part corresponding to stagnation flow over a flat plate and a small-disturbance part. Equation (2.1) demands that any linear disturbance must vary sinusoidally with the spanwise distance. Hence, we can express the flow quantities as

$$\left.\begin{aligned} u(X,y,z) &= X[U(y) + \epsilon\bar{u}(y)\sin(\alpha z) + O(\epsilon^2)], \\ v(X,y,z) &= \frac{1}{Re}[V(y) + \epsilon\bar{v}(y)\sin(\alpha z) + O(\epsilon^2)], \\ w(X,y,z) &= \frac{1}{Re}[\epsilon\bar{w}(y)\cos(\alpha z) + O(\epsilon^2)], \\ p_0 - p(X,y,z) &= \tfrac{1}{2}X^2 + \frac{1}{Re^2}[G(y) - \epsilon\bar{p}(y)\sin(\alpha z) + O(\epsilon^2)], \\ T(X,y,z) &= T(y) + \epsilon\bar{\Theta}(y)\sin(\alpha z) + O(\epsilon^2), \end{aligned}\right\} \tag{2.2}$$

where the X-dependence of the flow variables has been explicitly separated. Here (u, v, w) are velocity components in the (x, y, z) directions respectively; p denotes pressure, $p_0 = p(0, 0, z)$ when $\epsilon = 0$; (U, V) are undisturbed velocity components in the (x, y)-directions respectively; $(\bar{u}, \bar{v}, \bar{w})$ are amplitudes of the disturbance velocity components in the (x, y, z) directions respectively; G denotes the pressure distribution of the undisturbed flow; $\bar{p}$ is an amplitude of the pressure disturbance; and T, $\bar{\Theta}$ are the temperature of the undisturbed fluid and an amplitude of the temperature

disturbance, respectively. In the above, ϵ denotes the roughness amplitude and serves as an expansion parameter. It is very helpful to follow the behaviour of the x-component (streamwise) of vorticity, especially in view of the existence of the vorticity amplification mechanism. We shall call this component Ω and we shall refer to it as just 'vorticity' in the rest of the paper:

$$\Omega(X,y,z) = \frac{\partial w}{\partial y} - \frac{\partial v}{\partial z} = \frac{1}{Re}\left[\epsilon\left(\frac{\mathrm{d}\bar{w}}{\mathrm{d}y} - \alpha\bar{v}\right)\cos(\alpha z) + O(\epsilon^2)\right]. \tag{2.3}$$

Substituting (2.2) into the incompressible, constant-properties Navier–Stokes and continuity equations and the equation for energy transport without dissipation, and keeping only linear disturbance terms, we can express the field equations in the form:

basic flow

$$\frac{\mathrm{d}^2U}{\mathrm{d}y^2} - V\frac{\mathrm{d}U}{\mathrm{d}y} - U^2 + 1 = 0, \quad \frac{\mathrm{d}G}{\mathrm{d}y} = -\frac{\mathrm{d}^2V}{\mathrm{d}y^2} + V\frac{\mathrm{d}V}{\mathrm{d}y}, \tag{2.4a, b}$$

$$U + \frac{\mathrm{d}V}{\mathrm{d}y} = 0, \quad \frac{\mathrm{d}^2T}{\mathrm{d}y^2} - Pr\,V\frac{\mathrm{d}T}{\mathrm{d}y} = 0; \tag{2.4c, d}$$

disturbance flow

$$\frac{\mathrm{d}^2\bar{u}}{\mathrm{d}y^2} - V\frac{\mathrm{d}\bar{u}}{\mathrm{d}y} - (2U + \alpha^2)\,\bar{u} = \frac{\mathrm{d}U}{\mathrm{d}y}\bar{v}, \tag{2.5a}$$

$$\frac{\mathrm{d}^2\bar{v}}{\mathrm{d}y^2} - V\frac{\mathrm{d}\bar{v}}{\mathrm{d}y} - \left(\frac{\mathrm{d}V}{\mathrm{d}y} + \alpha^2\right)\bar{v} = \frac{\mathrm{d}\bar{p}}{\mathrm{d}y}, \tag{2.5b}$$

$$\frac{\mathrm{d}^2\bar{w}}{\mathrm{d}y^2} - V\frac{\mathrm{d}\bar{w}}{\mathrm{d}y} - \alpha^2\bar{w} = \alpha\bar{p}, \quad \bar{u} + \frac{\mathrm{d}\bar{v}}{\mathrm{d}y} - \alpha\bar{w} = 0, \tag{2.5c, d}$$

$$\frac{\mathrm{d}^2\bar{\Theta}}{\mathrm{d}y^2} - Pr\,V\frac{\mathrm{d}\bar{\Theta}}{\mathrm{d}y} - \alpha^2\bar{\Theta} = Pr\,\bar{v}\frac{\mathrm{d}T}{\mathrm{d}y}. \tag{2.5e}$$

We also have

$$\bar{\Omega} = \frac{\mathrm{d}\bar{w}}{\mathrm{d}y} - \alpha\bar{v}, \quad \frac{\mathrm{d}^2\bar{\Omega}}{\mathrm{d}y^2} - V\frac{\mathrm{d}\bar{\Omega}}{\mathrm{d}y} - \left(\alpha^2 + \frac{\mathrm{d}V}{\mathrm{d}y}\right)\bar{\Omega} = 0. \tag{2.6a, b}$$

In the above, Pr denotes the Prandtl number. Note that (2.4a–c) are decoupled from (2.4d) and (2.5a–d) are decoupled from (2.5e).

At the wall the no-slip and no-penetration conditions yield the boundary conditions

$$U = V = 0 \quad \text{at} \quad y = 0, \tag{2.7}$$

$$\bar{u} = -\frac{\mathrm{d}U}{\mathrm{d}y}, \quad \bar{v} = 0, \quad \bar{w} = 0 \quad \text{at} \quad y = 0, \tag{2.8}$$

where the condition for $\bar{v}$ has been simplified by application of (2.4c). For the temperature field, we assume either an isothermal plate,

$$T = 0 \quad \text{at} \quad y = 0, \tag{2.9}$$

$$\bar{\Theta} = -\frac{\mathrm{d}T}{\mathrm{d}y} \quad \text{at} \quad y = 0, \tag{2.10}$$

or a plate with a constant heat transfer rate

$$\frac{\mathrm{d}T}{\mathrm{d}y} = 1 \quad \text{at} \quad y = 0, \tag{2.11}$$

$$\frac{\mathrm{d}\bar{\Theta}}{\mathrm{d}y} = 0 \quad \text{at} \quad y = 0, \tag{2.12}$$

where the condition (2.12) has been simplified by applying (2.4d) and (2.7). In arriving at these boundary conditions, the actual boundary conditions were transferred to the mean position of the plate. This is justified when the roughness amplitude is small compared with the boundary-layer thickness ($\epsilon \ll 1$) and the thickness of the disturbance layer ($\alpha\epsilon \ll 1$). Far away from the plate the flow approaches potential isothermal stagnation flow and the effects of surface roughness become negligible, hence

$$U \to 1 \quad \text{as} \quad y \to \infty, \tag{2.13}$$

$$T \to 0 \quad \text{as} \quad y \to \infty, \tag{2.14}$$

$$\bar{u} \to 0, \quad \bar{v} \to 0, \quad \bar{w} \to 0 \quad \text{as} \quad y \to \infty, \tag{2.15}$$

$$\bar{\Theta} \to 0 \quad \text{as} \quad y \to \infty. \tag{2.16}$$

The additional stresses at the wall due to the presence of the roughness have the form

$$\left.\begin{aligned} \Delta\sigma_{yy} &= \frac{1}{Re^2}[-\bar{p}(0)+a]\sin(\alpha z), \\ \Delta\sigma_{yz} &= \frac{1}{Re^2}\frac{\mathrm{d}w}{\mathrm{d}y}\bigg|_{y=0}\cos(\alpha z), \\ \Delta\sigma_{yx} &= \frac{1}{Re}X\left(\frac{\mathrm{d}\bar{u}}{\mathrm{d}y}\bigg|_{y=0} - 1\right)\sin(\alpha z), \end{aligned}\right\} \tag{2.17}$$

where ρV_∞^2 has been used as the appropriate scale and $a = \mathrm{d}U/\mathrm{d}y|_{y=0}$. The increase of the heat flow at the surface in the case of an isothermal plate is given as

$$\Delta q_n = -\epsilon\frac{\mathrm{d}\bar{\Theta}}{\mathrm{d}y}\bigg|_{y=0}\sin(\alpha z), \tag{2.18}$$

where q_n is the heat flux in the direction normal to the plate. The modification of the wall temperature in the case of a plate with a constant heat flux is given as

$$\Delta T_w = \epsilon[1+\bar{\Theta}(0)]\sin(\alpha z). \tag{2.19}$$

3. Flow over a smooth plate

Stagnation flow over a smooth plate ($\epsilon = 0$) is described by (2.4a–c) with boundary conditions (2.7) and (2.13); this is the Hiemenz solution of the two-dimensional Navier–Stokes equations. Here we summarize results required for the analysis of roughness effects. We introduce a stream function f

$$U = \frac{\mathrm{d}f}{\mathrm{d}y}, \quad V = -f, \tag{3.1}$$

which leads to the boundary-value problem

$$\frac{\mathrm{d}^3 f}{\mathrm{d}y^3}+f\frac{\mathrm{d}^2 f}{\mathrm{d}y^2}-\left(\frac{\mathrm{d}f}{\mathrm{d}y}\right)^2+1=0, \tag{3.2}$$

$$\frac{\mathrm{d}G}{\mathrm{d}y}=\frac{\mathrm{d}^2 f}{\mathrm{d}y^2}+f\frac{\mathrm{d}f}{\mathrm{d}y}, \tag{3.3}$$

$$f=\frac{\mathrm{d}f}{\mathrm{d}y}=G=0 \quad \text{at} \quad y=0, \tag{3.4}$$

$$\frac{\mathrm{d}f}{\mathrm{d}y}\to 1 \quad \text{as} \quad y\to\infty. \tag{3.5}$$

The behaviour of the stream function in the neighbourhood of the plate ($y\to 0$) is given as

$$f=\tfrac{1}{2}ay^2-\tfrac{1}{6}y^3+\frac{a^2}{120}y^5+O(y^6), \tag{3.6}$$

where $a=\mathrm{d}U/\mathrm{d}y|_{y=0}=1.232587$ has been determined by numerical integration. According to (3.5), the behaviour of the stream function far away from the wall ($y\to\infty$) is approximated as

$$f\to Y+\Phi(Y), \tag{3.7}$$

where $Y=y-A$, $A=0.6479004$ has been determined by numerical integration and the function $\Phi(Y)\to 0$ as $Y\to\infty$ and describes the rate at which f approaches its asymptotic form. The form of Φ is obtained by substituting (3.7) into (3.2) and linearizing for small Φ. This results in an equation

$$\frac{\mathrm{d}^3\Phi}{\mathrm{d}Y^3}+Y\frac{\mathrm{d}^2\Phi}{\mathrm{d}Y^2}-2\frac{\mathrm{d}\Phi}{\mathrm{d}Y}=0 \tag{3.8}$$

whose solution involves integrals of parabolic cylinder functions and a constant. The solution that satisfies the conditions for $y\to\infty$ leads to the stream function in a form

$$f=Y+c_1[-Y^{-4}+10Y^{-6}-105Y^{-8}+O(Y^{-10})]\mathrm{e}^{-\frac{1}{2}Y^2}, \tag{3.9}$$

where the constant $c_1=-0.645$ has been determined by matching of (3.9) with a numerical solution inside the boundary layer. We note a very rapid approach of the stream function to its asymptotic form with an increase of distance away from the plate.

The temperature field associated with a stagnation flow over a smooth plate ($\epsilon=0$) is described by (2.4*d*) with boundary condition (2.14) and one of either (2.9) or (2.11). The solution has the form

$$T=1-B\int_0^y \exp\left(Pr\int_0^y V\,\mathrm{d}y\right)\mathrm{d}y \tag{3.10}$$

in the case of an isothermal plate, and

$$T=-B^{-1}+\int_0^y \exp\left(Pr\int_0^y V\,\mathrm{d}y\right)\mathrm{d}y \tag{3.11}$$

in the case of a constant-heat-flux plate. The constant B is defined as

$$B^{-1} = \int_0^\infty \exp\left(\int_0^y Pr\, V\, \mathrm{d}y\right) \mathrm{d}y \tag{3.12}$$

and has been tabulated for a few values of Prandtl number in Goldstein (1938). Explicit results are given in the present paper for a flow of air ($Pr = 0.71$) and a flow of water ($Pr = 7.0$) for which $B = 0.4986628$ and 1.178375 respectively. Variations of temperature in the neighbourhood of an isothermal plate are given as

$$T = 1 - B[y - \tfrac{1}{24} a\, Pr\, y^4 + \tfrac{1}{120} Pr\, y^5 + O(y^6)], \quad y \to 0, \tag{3.13}$$

and in the neighbourhood of a plate with a fixed heat flux

$$T = -B^{-1} + y - \tfrac{1}{24} a\, Pr\, y^4 + \tfrac{1}{120} Pr\, y^5 + O(y^6), \quad y \to 0. \tag{3.14}$$

Variations of temperature outside the flow boundary layer and far away from the plate can be approximated as

$$T = c_2[-Pr^{-1}Y^{-1} + Pr^{-2}Y^{-3} - 3Pr^{-3}Y^{-5} + O(Y^{-7})]\, \mathrm{e}^{-\frac{1}{2}PrY^2}, \quad Y \to \infty \tag{3.15}$$

for both types of plates. The constant c_2 has been determined by matching of (3.15) with a numerical solution of (2.4d) inside the boundary layer; $c_2 = -0.448$, -0.414 in the case of an isothermal plate with $Pr = 0.71$, 7.0 respectively, and $c_2 = 0.899$, 0.351 in the case of a constant-heat-flux plate with $Pr = 0.71$, 7.0 respectively. We note again a very rapid approach to the asymptotic state with an increase of distance away from the plate.

4. Disturbance flow

Modifications of the flow field caused by surface roughness are described by (2.5a–d) with boundary conditions (2.8) and (2.15). A general solution, valid for arbitrary values of the parameters, can be found only numerically and the appropriate procedure is described in §4.1. Explicit solutions, which have been found in the asymptotic limits of $\alpha \to 0$ and $\alpha \to \infty$ are described in §§4.2 and 4.3 respectively.

4.1. *Numerical procedure*

The functional form of the solution of the system (2.5) for large values of y can be determined explicitly. It is then sufficient to carry out the numerical calculation between $y = 0$ and y large enough for the asymptotic solution to be valid.

In the limit $y \to \infty$, the basic flow assumes asymptotic form (3.7) and the disturbance equations simplify to the form.

$$\frac{\mathrm{d}^2\bar{u}}{\mathrm{d}Y^2} + Y\frac{\mathrm{d}\bar{u}}{\mathrm{d}Y} - (\alpha^2+2)\,\bar{u} = 0, \quad \frac{\mathrm{d}^2\bar{v}}{\mathrm{d}Y^2} + Y\frac{\mathrm{d}\bar{v}}{\mathrm{d}Y} - (\alpha^2-1)\,\bar{v} = \frac{\mathrm{d}\bar{p}}{\mathrm{d}Y}, \tag{4.1a, b}$$

$$\frac{\mathrm{d}^2\bar{w}}{\mathrm{d}Y^2} + Y\frac{\mathrm{d}\bar{w}}{\mathrm{d}Y} - \alpha^2\bar{w} = \alpha\bar{p}, \quad \bar{u} + \frac{\mathrm{d}\bar{v}}{\mathrm{d}Y} - \alpha\bar{w} = 0, \tag{4.1c, d}$$

where the effects of the function Φ have been assumed to be negligible. We note that the coupling between the x-momentum, (2.5a), and the rest of the system is proportional to $\mathrm{d}^2\Phi/\mathrm{d}Y^2$ and is neglected in the above approximation. Equation (4.1a) can be solved independently and its solution is expressible as a superposition of linearly independent parabolic cylinder functions. The explicit forms of these functions valid for large values of the independent variable can be found in

Abramowitz & Stegun (1965). In the limit $Y \to \infty$, the solution of (4.1*a*) that satisfies the condition (2.15) has the form

$$\bar{u} \sim b_1 \mathrm{e}^{-\frac{1}{2}Y^2} Y^{-\alpha^2} \{Y^{-3} - \tfrac{1}{2}(3+\alpha^2)(4+\alpha^2) Y^{-5} + \tfrac{1}{8}(3+\alpha^2)(4+\alpha^2)(5+\alpha^2)(6+\alpha^2) Y^{-7} + O(Y^{-9})\}, \quad (4.2)$$

where b_1 is an arbitrary constant. It is simpler to discuss the solution of the rest of the system by considering the x-component of vorticity first. The governing equation has the form

$$\frac{\mathrm{d}^2\bar{\Omega}}{\mathrm{d}Y^2} + Y\frac{\mathrm{d}\bar{\Omega}}{\mathrm{d}Y} - (\alpha^2 - 1)\bar{\Omega} = 0 \quad (4.3)$$

and its solution, which involves parabolic cylinder functions, can be expressed for $Y \to \infty$ as

$$\bar{\Omega} \sim b_3 \mathrm{e}^{-\frac{1}{2}Y^2} Y^{-\alpha^2}[1 + O(Y^{-2})] + b_4 Y^{\alpha^2 - 1}[1 + O(Y^{-2})]. \quad (4.4)$$

When $\alpha \geqslant 1$, the solution proportional to constant b_4 does not satisfy the boundary conditions for $Y \to \infty$ and has to be rejected, i.e. $b_4 = 0$. When $\alpha < 1$, the boundary conditions are formally satisfied by both linearly independent solutions and this leads in a non-unique solution of the disturbance equations. The situation is analogous to the one found in the analysis of the stability of stagnation flow (Wilson & Gladwell 1978). It is resolved there by requiring the solutions to decay exponentially outside the boundary layer. The arguments put forward are: (i) since the main-stream vorticity decays exponentially outside the boundary layer, any disturbance vorticity that originates inside the boundary layer also has to decay outside the boundary layer exponentially, and (ii) the acceptance of the algebraically decaying term should lead to inconsistencies in the matching procedure between the inner and the outer flows at the higher level of approximation. The second argument has been put forward only in a qualitative form. The first argument clearly applies in the present case; the disturbance vorticity originates at the wall and it can penetrate upstream only by diffusion, hence it is natural to require exponential decay. The approaching flow contains no disturbances and, therefore, there is no need to speculate about their evolution as they approach the plate, i.e. there is no need to maintain algebraically varying terms. In addition, we expect the roughness effects to be qualitatively similar regardless of whether $\alpha \geqslant 1$ or $\alpha < 1$. Thus, we consider the part of the solution proportional to b_4 to be physically irrelevant and, accordingly, we set $b_4 = 0$. The conjecture about exponential decay of the disturbances is also supported by the results obtained in §4.3 in the limit $\alpha \to \infty$ where the exponential decay comes explicitly out of the analysis.

We obtain an equation for $\bar{w}$ by combining (4.1*d*) and (2.6*a*):

$$\frac{\mathrm{d}^2\bar{w}}{\mathrm{d}Y^2} - \alpha^2\bar{w} = \frac{\mathrm{d}\bar{\Omega}}{\mathrm{d}Y} + \alpha\bar{u}. \quad (4.5)$$

The homogeneous part of (4.5) brings in the solutions of the type $\mathrm{e}^{\alpha Y}$ and $\mathrm{e}^{-\alpha Y}$, with the former to be rejected in view of (2.5). The inhomogeneous part of (4.5) can be determined by standard methods. The pressure and $\bar{v}$-component can be determined by substitution into one of the field equations. The results for $\bar{v}$, $\bar{w}$, $\bar{p}$ and $\bar{\Omega}$ fields that contain only exponentially decaying vorticity for $Y \to \infty$ and satisfy all the boundary conditions (2.15) are

$$\bar{v} \sim -b_5 \mathrm{e}^{-\alpha Y} - b_3 \alpha \mathrm{e}^{-\frac{1}{2}Y^2} Y^{-\alpha^2} \{-Y^{-2} + \tfrac{1}{2}(\alpha^4 + 3\alpha^2 + 6) Y^{-4} + O(Y^{-6})\} + b_1 \mathrm{e}^{-\frac{1}{2}Y^2} Y^{-\alpha^2} \{Y^{-4} + O(Y^{-6})\}, \quad (4.6a)$$

$$\bar{w} \sim b_5 \mathrm{e}^{-\alpha Y} + b_3 \mathrm{e}^{-\frac{1}{2}Y^2} Y^{-\alpha^2} \{ -Y^{-1} + \tfrac{1}{2}(\alpha^4 + \alpha^2 + 2)\, Y^{-3} - [\tfrac{1}{8}\alpha^2(\alpha^2+1)(\alpha^2+2)(\alpha^2+3) + \tfrac{1}{2}(\alpha^4+\alpha^2+6)]\, Y^{-5} + O(Y^{-7}) \} - b_1 \alpha \mathrm{e}^{-\frac{1}{2}Y^2} Y^{-\alpha^2} \{ Y^{-5} + O(Y^{-1}) \}, \tag{4.6b}$$

$$\bar{P} \sim -b_5 Y^{-\alpha Y} - b_3 2\alpha \mathrm{e}^{-\frac{1}{2}Y^2} Y^{-\alpha^2} \{ Y^{-3} + O(Y^{-5}) \} - b_1 4 \mathrm{e}^{-\frac{1}{2}Y^2} Y^{-\alpha^2} \{ Y^{-5} + O(Y^{-7}) \}, \tag{4.6c}$$

$$\bar{\Omega} \sim b_3 \mathrm{e}^{-\frac{1}{2}Y^2} Y^{-\alpha^2} \{ 1 - \tfrac{1}{2}\alpha^2(\alpha^2+1)\, Y^{-2} + \tfrac{1}{8}\alpha^2(\alpha^2+1)(\alpha^2+2)(\alpha^2+3)\, Y^{-4} + O(Y^{-6}) \}, \tag{4.6d}$$

where b_1, b_3, b_5 are arbitrary constants to be determined from matching with a numerical solution inside the boundary layer. We note that parts of the solution proportional to b_1 and b_5 produce no vorticity.

Modifications of the temperature field caused by surface roughness are described by (2.5*e*) with boundary condition (2.16) and one of either (2.10) or (2.12). In the limit $Y \to \infty$, outside the flow and thermal boundary layers, the disturbance equation reduces to

$$\frac{\mathrm{d}^2\bar{\Theta}}{\mathrm{d}Y^2} + Pr\, Y \frac{\mathrm{d}\bar{\Theta}}{\mathrm{d}Y} - \alpha^2 \bar{\Theta} = 0. \tag{4.7}$$

The solution involves parabolic cylinder functions and the part that satisfies (2.16) can be approximated as

$$\bar{\Theta} \sim b_7 \mathrm{e}^{-\frac{1}{2}PrY^2} (Pr^{\frac{1}{2}}Y)^{-(\alpha^2/Pr)-1} \left\{ 1 - \frac{(\alpha^2/Pr+1)(\alpha^2/Pr+2)}{2Pr} Y^{-2} + \frac{(\alpha^2/Pr+1)(\alpha^2/Pr+2)(\alpha^2/Pr+3)(\alpha^2/Pr+4)}{8Pr^2} Y^{-4} + O(Y^{-6}) \right\}. \tag{4.8}$$

We note that $Y \gg Pr^{-\frac{1}{2}}$ for the above approximation to hold.

For the purpose of numerical calculations we replace (2.5) with a system of first-order differential equations. Here we consider $s_1 = u$, $s_2 = \mathrm{d}\bar{u}/\mathrm{d}y$, $s_3 = \bar{v}$, $s_4 = \bar{w}$, $s_5 = \mathrm{d}\bar{w}/\mathrm{d}y$, $s_6 = \bar{p}$ to be unknowns. At a sufficiently large y, we assume that the first term in the asymptotic series dominates and, accordingly, we assume the boundary conditions to be in the form

$$s_1 = -Ys_1, \quad s_5 = -\alpha s_4, \quad s_6 = Ys_3. \tag{4.9a–c}$$

It has been found through experimentation that it was sufficient to apply these boundary conditions at y no larger than 7.5 for the smallest value of wavenumber considered. When α was sufficiently large, the boundary conditions (2.15) were applied directly at a finite y without resorting to the asymptotic solution. This procedure has been followed for $\alpha > 4$ with boundary conditions applied at y no larger than 4. As a check, an alternative system has been formed, where $\bar{s}_1 = \bar{u}$, $\bar{s}_2 = \mathrm{d}\bar{u}/\mathrm{d}y$, $\bar{s}_3 = \bar{v}$, $\bar{s}_4 = \mathrm{d}\bar{v}/\mathrm{d}y$, $\bar{s}_5 = \mathrm{d}^2\bar{v}/\mathrm{d}y^2$, $\bar{s}_6 = \mathrm{d}^3\bar{v}/\mathrm{d}y^3$ were considered to be unknown. The appropriate boundary conditions for large y were

$$\bar{s}_2 = -Y\bar{s}_1, \quad \bar{s}_4 = -\alpha\bar{s}_3, \quad \bar{s}_5 = -\alpha\bar{s}_4. \tag{4.10a–c}$$

Results obtained with both formulations agreed. As a further check, numerical results were compared with the analytical solutions obtained in the limits of $\alpha \to 0$ and $\alpha \to \infty$. Again, a very good agreement was noted.

When the temperature field was desired, the original set of equations was supplemented by $s_7 = \bar{\Theta}$, $s_8 = \mathrm{d}\bar{\Theta}/\mathrm{d}y$ with boundary conditions at large y in the form

$$s_8 = -Pr\, Y s_7. \tag{4.11}$$

The temperature and velocity fields were then calculated simultaneously.

The numerical algorithm used to solve the boundary-value problem involved varible-step-size finite-difference discretization with deferred corrections (Pereyra 1979). The resulting algebraic system was solved by Gauss elimination.

4.2. *Small-wavenumber limit* ($\alpha \to 0$)

The purpose of the analysis described in this section is to elucidate the structure of the disturbance field in the limit $\alpha \to 0$. Since the thickness of the disturbance layer is $O(\alpha^{-1})$, in the limit it becomes large compared with the thickness of the flow boundary layer. The disturbance flow field can then be qualitatively divided into an outer part, which overlaps the potential flow, and an inner part or a disturbance boundary layer, which is induced by and overlaps the flow boundary layer.

The limit $\alpha \to 0$ should not be interpreted as the one corresponding to a smooth plate. No matter how small α is, one can always find z large enough to make $\alpha z = O(1)$ in (2.1) and thus to retain the spanwise periodicity of the flow. The results presented in this section should be viewed as describing a universal structure of the disturbance flow field for small but finite α.

We begin the analysis by looking at the outer part of the disturbance layer. The character of the solution can be deducted from (4.2) and (4.6), which suggest that $\bar{u}(\sim Y^{-3}\mathrm{e}^{-\frac{1}{2}Y^2})$ is negligibly small compared with $\bar{v}$, $\bar{w}$, $\bar{p}(\sim \mathrm{e}^{-\alpha Y})$ and can be dropped from the continuity equation (4.1*d*). The set of equations to be considered is

$$\frac{\mathrm{d}^2\bar{v}}{\mathrm{d}Y^2} + Y\frac{\mathrm{d}\bar{v}}{\mathrm{d}Y} - (\alpha^2 - 1) = \frac{\mathrm{d}\bar{p}}{\mathrm{d}Y}, \quad \frac{\mathrm{d}^2\bar{w}}{\mathrm{d}Y^2} + Y\frac{\mathrm{d}\bar{w}}{\mathrm{d}Y} - \alpha^2\bar{w} = \alpha\bar{p}, \tag{4.12a, b}$$

$$\frac{\mathrm{d}^2\bar{v}}{\mathrm{d}Y^2} - \alpha\bar{w} = 0. \tag{4.12c}$$

One could carry out the required asymptotic analysis of (4.12); however, here we take advantage of the information contained in (4.6). The dominant solution is proportional to b_5; it is an exact solution of (4.12) and it is good for any value of Y and α. The solution proportional to b_1, which appears to be due to coupling with $\bar{u}$, does not arise in (4.12). Thus, in the limit $\alpha \to 0$, the disturbances assume the form

$$\bar{u} \approx 0, \quad \bar{v} \approx -b_5\,\mathrm{e}^{-\alpha Y}, \quad \bar{w} \approx -\bar{v}, \quad \bar{p} \approx Y\bar{v}, \quad \bar{\Omega} \approx 0, \tag{4.13}$$

where the omitted terms have the rate of decay at least proportional to $\mathrm{e}^{-\frac{1}{2}Y^2}$. To determine the character of the solution at the edge of the flow boundary layer, we take the limit $\alpha \to 0$, $Y = O(1)$ and fixed, and replace the exponential functions in (4.13) with the appropriate expansions. Thus we obtain

$$\bar{v} \approx -b_5[1 - \alpha Y + \tfrac{1}{2}\alpha^2 Y^2 + O(\alpha^3)], \tag{4.14}$$

where b_5 is an arbitrary constant to be determined by matching with the solution originating inside the flow boundary layer, and $\bar{u}$, $\bar{w}$, $\bar{p}$ and $\bar{\Omega}$ are given by (4.13).

We assume the solution inside the flow boundary layer to have the form

$$\bar{q} = q_0 + \alpha q_1 + O(\alpha^2), \tag{4.15}$$

where q denotes any flow quantity. Substitution of (4.15) into (2.5a–d) and (2.8) results in

$$L_1(u_0, v_0, w_0, p_0) \equiv \frac{\mathrm{d}^2 u_0}{\mathrm{d}y^2} - V\frac{\mathrm{d}u_0}{\mathrm{d}y} - 2Uu_0 - \frac{\mathrm{d}U}{\mathrm{d}y}v_0 = 0, \tag{4.16a}$$

$$L_2(u_0, v_0, w_0, p_0) \equiv \frac{\mathrm{d}^2 v_0}{\mathrm{d}y^2} - V\frac{\mathrm{d}v_0}{\mathrm{d}y} - \frac{\mathrm{d}V}{\mathrm{d}y}v_0 - \frac{\mathrm{d}p_0}{\mathrm{d}y} = 0, \tag{4.16b}$$

$$L_3(u_0, v_0, w_0, p_0) \equiv \frac{\mathrm{d}^2 w_0}{\mathrm{d}y^2} - V\frac{\mathrm{d}w_0}{\mathrm{d}y} = 0, \tag{4.16c}$$

$$L_4(u_0, v_0, w_0, p_0) \equiv u_0 + \frac{\mathrm{d}v_0}{\mathrm{d}y} = 0, \tag{4.16d}$$

$$u_0 = -\frac{\mathrm{d}U}{\mathrm{d}y}, \quad v_0 = 0, \quad w_0 = 0 \quad \text{at} \quad y = 0, \tag{4.16e}$$

$$L_1(u_1, v_1, w_1, p_1) = 0, \quad L_2(u_1, v_1, w_1, p_1) = 0, \tag{4.17a, b}$$

$$L_3(u_1, v_1, w_1, p_1) = p_0, \quad L_4(u_1, v_1, w_1, p_1) = w_0, \tag{4.17c, d}$$

$$u_1 = 0, \quad v_1 = 0, \quad w_1 = 0 \quad \text{at} \quad y = 0. \tag{4.17e}$$

It is a simple matter to write equations for higher-order corrections. Equation (4.16c) decouples and has a general solution in the form

$$w_0 = d_1 \int \exp\left(\int V\,\mathrm{d}y\right)\mathrm{d}y + d_2, \tag{4.18}$$

where d_1, d_2 are constants to be determined from the boundary condition at $y = 0$ and from matching with (4.13) and (4.14) outside the flow boundary layer. Elimination of u_0 and p_0 from (4.16a, b, d) results in

$$\frac{\mathrm{d}^3 v_0}{\mathrm{d}y^3} - V\frac{\mathrm{d}^2 v_0}{\mathrm{d}y^2} - 2U\frac{\mathrm{d}v_0}{\mathrm{d}y} + \frac{\mathrm{d}U}{\mathrm{d}y}v_0 = 0 \tag{4.19}$$

whose solution satisfying the boundary condition (4.16e) is

$$v_0 = U. \tag{4.20}$$

This can be demonstrated by taking $\mathrm{d}/\mathrm{d}y$ of (2.4a) and using (2.4c), which leads to an equation identical to (4.19). Equations (4.20) and (4.16d) imply

$$u_0 = -\frac{\mathrm{d}U}{\mathrm{d}y} \tag{4.21}$$

and this result is consistent with the boundary conditions (4.16e). It can be shown in an analogous manner that

$$p_0 = \frac{\mathrm{d}G}{\mathrm{d}y} + d_3 = \frac{\mathrm{d}U}{\mathrm{d}y} - VU + d_3, \tag{4.22}$$

where d_3 is a constant to be determined from matching.

Matching involves only v_0, w_0 and p_0, since $\bar{u}$ is considered negligibly (exponentially) small outside the flow boundary layer. The component u_0 indeed decays exponentially, however at a rate slightly different from the complete solution given by (4.2). This is of no concern since u_0 approximates $\bar{u}$ only inside the flow boundary layer, while outside $\bar{u} \approx 0$. It is perhaps simplest to demonstrate matching

by beginning with v_0. In the limit $y \to \infty$, $v_0 \approx 1$ and matching with the term $O(\alpha^0)$ in (4.13) and (4.14) requires setting $b_5 = -1$. Pressure matching requires $d_3 = 0$, and matching of $\bar{w}$ results in

$$w_0 = -D \int_0^y \exp\left(\int_0^y V \, dy \right) dy, \tag{4.23}$$

where

$$D^{-1} = \int_0^\infty \exp\left(\int_0^y V \, dy \right) dy = 0.5704653^{-1},$$

which is similar to the expression for the basic temperature field with $Pr = 1.0$. The expression for vorticity is

$$\Omega_0 = \frac{dw_0}{dy} = -D \exp\left(\int_0^y V \, dy \right). \tag{4.24}$$

It is interesting to note that a non-trivial solution of the disturbance equations exists because of an inhomogeneous boundary condition for $\bar{u}$ at the wall, (2.8); this is where the forcing term is. Inside the flow boundary layer in the limit $\alpha \to 0$ this forcing affects directly only u_0, v_0 and p_0, while w_0, which is the only component giving rise to a streamwise vorticity, is driven by a coupling that exists only outside the flow boundary layer and has a vorticity-free character, e.g. (4.13).

Corrections of $O(\alpha)$ are described by (4.17), where (4.17*c*) is decoupled. The explicit form of (4.17*c*) is

$$\frac{dw_1}{dy^2} - V \frac{dw_1}{dy} = \frac{dU}{dy} - VU \tag{4.25}$$

and leads to a solution

$$w_1 = -V, \tag{4.26}$$

which is consistent with the boundary condition (4.17*e*) and matches with (4.13) and (4.14). It is interesting to note that

$$\Omega_1 = \frac{dw_1}{dy} - v_0 = 0. \tag{4.27}$$

One can eliminate u_1 and p_1 from (4.17*a*, *b*, *d*) and obtain

$$\frac{d^3 v_1}{dy^3} - V \frac{d^2 v_1}{dy^2} - 2U \frac{dv_1}{dy} + \frac{dU}{dy} v_1 = -2U w_0, \tag{4.28a}$$

where the appropriate boundary conditions are

$$v_1 = \frac{dv_1}{dy} = 0 \quad \text{at} \quad y = 0, \quad \frac{dv_1}{dy} = -1 \quad \text{at} \quad y \to \infty. \tag{4.28b, c}$$

The condition (4.28*c*) comes from the matching with (4.13) and (4.14). Solution of (4.28) requires numerical work. Component u_1 can be determined from (4.17*d*) with v_1 known; it is easy to show without solving that the matching condition for u_1 is satisfied. The equation for the pressure p_1 is

$$\frac{dp_1}{dy} = \frac{d^2 v_1}{dy^2} - \frac{d}{dy}(V v_1) \tag{4.29}$$

and again it is easy to show without solving that the matching condition is satisfied. One could carry out a similar analysis for the corrections of $O(\alpha^2)$ and higher. It is not described here since no explicit solutions have been found.

It is instructive to write uniformly valid, i.e. composite, expansions for the flow components. Following standard methods (Nayfeh 1973) one obtains

$$\bar{u} = -\frac{\mathrm{d}U}{\mathrm{d}y} + O(\alpha), \quad \bar{v} = U + \mathrm{e}^{-\alpha y} - 1 + O(\alpha), \tag{4.30a, b}$$

$$\bar{w} = -D\int_0^y \exp\left(\int_0^y V\,\mathrm{d}y\right)\mathrm{d}y - \mathrm{e}^{-\alpha y} + 1 + \alpha[-V - A\,\mathrm{e}^{-\alpha y} + A - y] + O(\alpha^2), \tag{4.30c}$$

$$\bar{p} = \frac{\mathrm{d}U}{\mathrm{d}y} - VU + (y - A)\,\mathrm{e}^{-\alpha y} - y + A + O(\alpha), \tag{4.30d}$$

$$\bar{\Omega} = -D\exp\left(\int_0^y V\,\mathrm{d}y\right) + O(\alpha^2). \tag{4.30e}$$

The limiting values of the wall stresses can be deduced by noting that $\bar{p} \to a$, $\mathrm{d}\bar{w}/\mathrm{d}y \to -D$, $\mathrm{d}\bar{u}/\mathrm{d}y \to 1$ when $\alpha \to 0$. Here D is given by (4.23).

The behaviour of the disturbance temperature field outside the flow boundary layer is given by (4.8), which shows that the temperature disturbance is negligible (exponentially) small there. We assume the solution to have the form (4.15) inside the flow boundary layer, which leads to the following equation at the leading order of approximation:

$$\frac{\mathrm{d}^2\Theta_0}{\mathrm{d}y^2} - Pr\,V\frac{\mathrm{d}\Theta_0}{\mathrm{d}y} - Pr\frac{\mathrm{d}T}{\mathrm{d}y}v_0 = 0, \tag{4.31a}$$

$$\Theta_0 = -\frac{\mathrm{d}T}{\mathrm{d}y} \quad \text{or} \quad \frac{\mathrm{d}\Theta_0}{\mathrm{d}y} = 0 \quad \text{at} \quad y = 0. \tag{4.31b}$$

Solution of (4.21a) has the form

$$\Theta_0 = -\frac{\mathrm{d}T}{\mathrm{d}y} \tag{4.32}$$

which can be demonstrated by taking $\mathrm{d}/\mathrm{d}y$ of (2.4d) and using (2.4c); the resulting equation is identical to (4.31a). The solution (4.32) satisfies the wall boundary conditions in the cases of both isothermal and constant-heat-flux walls. It decays exponentially outside the flow boundary layer, however at a rate slightly different from the complete solution (4.8). It is of no concern, as in the case of the approximation for $\bar{u}$, since Θ_0 approximates $\bar{\Theta}$ only inside the flow boundary layer, while outside $\bar{\Theta} \approx 0$. Thus (4.32) provides a uniformly valid approximation for $\bar{\Theta}$ with error $O(\alpha)$.

The limiting value of the increase of the heat flow at the surface of an isothermal plate can be deduced by noting that $\mathrm{d}\Theta/\mathrm{d}y|_{y=0} \to 0$ as $\alpha \to 0$, and the limiting value of the change of the wall temperature in the case of a plate with a constant heat flux is given by noting that $\bar{\Theta}(0) \to -1$ as $\alpha \to 0$.

4.3. *Large-wavenumber limit* ($\alpha \to \infty$)

The analysis described in this section explains the structure of the disturbance field in the limit $\alpha \to \infty$. In the limit, the thickness of the disturbance layer becomes small compared with the thickness of the flow boundary layer. The disturbance velocity field is then affected only by the properties of the mean flow in a small neighbourhood of the plate. As stated in §2, these results are valid only if $\alpha\epsilon \ll 1$, i.e. the height of the roughness has to be small compared with the thickness of the disturbance layer. The analysis has been carried out up to $O(\alpha^{-3})$ to demonstrate that a simple approximation obtained by replacing the mean velocity U by a linear function is actually $O(\alpha^{-3})$ accurate.

We begin the analysis by eliminating first derivatives of the dependent variables from the governing equations (2.5). Thus, we let

$$\bar{q}(y) = \tilde{q}(y) \exp\left(\frac{1}{2}\int_0^y V \,\mathrm{d}y\right), \tag{4.33}$$

where q denotes any flow quantity. Then we introduce a new independent variable

$$y_1 = \alpha y, \quad \frac{\mathrm{d}}{\mathrm{d}y} = \alpha \frac{\mathrm{d}}{\mathrm{d}y_1}, \quad \frac{\mathrm{d}^2}{\mathrm{d}y^2} = \alpha^2 \frac{\mathrm{d}^2}{\mathrm{d}y_1^2}, \tag{4.34}$$

which is equivalent to rescaling the field equations with respect to the disturbance wavelength as a lengthscale. We also let

$$\bar{p} = \alpha \hat{p}. \tag{4.35}$$

Since disturbances are confined to a thin layer next to the wall, coefficients in the equations can be replaced by their Taylor expansions around the wall. The resulting equations have the following form:

$$\frac{\mathrm{d}^2\tilde{u}}{\mathrm{d}y_1^2} + [-1 - \alpha^{-3\frac{5}{2}} a y_1 - \alpha^{-4\frac{5}{4}} y_1^2 + O(\alpha^{-6})]\,\tilde{u} = [\alpha^{-1} a - \alpha^{-3} y_1 + O(\alpha^{-5})]\,\tilde{v}, \tag{4.36a}$$

$$\frac{\mathrm{d}^2\tilde{v}}{\mathrm{d}y_1^2} + [-1 - \alpha^{-3\frac{1}{2}} a y_1 - \alpha^{-4\frac{1}{4}} y_1^2 + O(\alpha^{-6})]\,\tilde{v} = \frac{\mathrm{d}\hat{p}}{\mathrm{d}y_1} + [-\alpha^{-3\frac{1}{4}} a y_1^2 + \alpha^{-4\frac{1}{12}} y_1^3 + O(\alpha^{-6})]\,\hat{p}, \tag{4.36b}$$

$$\frac{\mathrm{d}^2\tilde{w}}{\mathrm{d}y_1^2} + [-1 - \alpha^{-3\frac{1}{2}} a y_1 + \alpha^{-4\frac{1}{4}} y_1^2 + O(\alpha^{-6})]\,\tilde{w} = \hat{p}, \tag{4.36c}$$

$$\alpha^{-1}\tilde{u} + \frac{\mathrm{d}\tilde{v}}{\mathrm{d}y_1} + [-\alpha^{-3\frac{1}{4}} a y_1^2 + \alpha^{-4\frac{1}{12}} y_1^3 + O(\alpha^{-6})]\,\tilde{v} - \tilde{w} = 0. \tag{4.36d}$$

We now assume all flow quantities to be in the form

$$q = q_0 + \alpha^{-1} q_1 + \alpha^{-2} q_2 + \alpha^{-3} q_3 + \alpha^{-4} q_4 + O(\alpha^{-5}) \tag{4.37}$$

and, after substituting (4.37) into (4.36), we obtain at the leading order of approximation

$$\hat{L}_1(u_0, v_0, w_0, p_0) \equiv \frac{\mathrm{d}^2 u_0}{\mathrm{d}y_1^2} - u_0 = 0, \tag{4.38a}$$

$$\hat{L}_2(u_0, v_0, w_0, p_0) \equiv \frac{\mathrm{d}^2 v_0}{\mathrm{d}y_1^2} - v_0 - \frac{\mathrm{d}\hat{p}_0}{\mathrm{d}y_1} = 0, \tag{4.38b}$$

$$\hat{L}_3(u_0, v_0, w_0, p_0) \equiv \frac{\mathrm{d}^2 w_0}{\mathrm{d}y_1^2} - w_0 - \hat{p}_0 = 0, \tag{4.38c}$$

$$\hat{L}_4(u_0, v_0, w_0, p_0) \equiv \frac{\mathrm{d}v_0}{\mathrm{d}y} - w_0 = 0, \tag{4.38d}$$

$$u_0 = -a, \quad v_0 = w_0 = 0 \quad \text{at} \quad y_1 = 0, \tag{4.38e}$$

$$u_0 \to 0, \quad v_0 \to 0, \quad w_0 \to 0 \quad \text{as} \quad y_1 \to \infty. \tag{4.38f}$$

Higher-order equations can be found in the Appendix. The relevant solutions are as follows:

$$u_0 = -a\,\mathrm{e}^{-y_1}, \quad v_0 = 0, \quad w_0 = 0, \quad \hat{p}_0 = 0, \tag{4.39}$$

$$u_1 = 0, \quad v_1 = a y_1 \mathrm{e}^{-y_1}, \quad w_1 = -a y_1 \mathrm{e}^{-y_1}, \quad \hat{p}_1 = 2a\,\mathrm{e}^{-y_1}, \tag{4.40}$$

$$u_2 = 0, \quad v_2 = 0, \quad w_2 = 0, \quad \hat{p}_2 = 0, \tag{4.41}$$

$$u_3 = \tfrac{3}{8}a^2 y_1(1+y_1)\,\mathrm{e}^{-y_1}, \quad v_3 = 0, \quad w_3 = 0, \quad \hat{p}_3 = 0, \tag{4.42}$$

where $a = \mathrm{d}U/\mathrm{d}y|_{y=0}$. These solutions lead to the complete approximation for $\bar{u}$, $\bar{v}$, $\bar{w}$, $\bar{p}$ and $\bar{\Omega}$ in the form

$$\bar{u} = [-a + \alpha^{-3}a^2 y_1(\tfrac{3}{8} + \tfrac{3}{8}y_1 + \tfrac{1}{12}y_1^2)]\,\mathrm{e}^{-y_1} + O(\alpha^{-4}), \tag{4.43a}$$

$$\bar{v} = \alpha^{-1} a y_1 \mathrm{e}^{-y_1} + O(\alpha^{-4}), \quad \bar{w} = -\alpha^{-1} a y_1 \mathrm{e}^{-y_1} + O(\alpha^{-4}), \tag{4.43b, c}$$

$$\bar{p} = 2a\,\mathrm{e}^{-y_1} + O(\alpha^{-3}), \quad \bar{\Omega} = -a\,\mathrm{e}^{-y_1} + O(\alpha^{-3}). \tag{4.43d, e}$$

One could carry out a similar analysis in terms of $\bar{u}$, $\bar{v}$, $\bar{w}$, $\bar{\Omega}$ and the same results would be obtained without making an explicit assumption regarding the magnitude of the pressure.

The basic flow affects the results only at the level $O(\alpha^{-3})$; here the coupling existing in the field equations at the level $O(\alpha^{-2})$ has been eliminated through imposition of the boundary conditions. Such elimination might not be possible when other types of boundary conditions like, for example, those corresponding to suction, are considered. It is interesting to note that in the present case U can be considered linear (and V parabolic) for approximations up to $O(\alpha^{-3})$ inclusive. This suggests that one could obtain acceptable results for α close to unity by working with the full disturbance equations (2.6) and a simplified, i.e. linear, basic flow. Such a simplification formed the basis of an analysis carried out by Lighthill (1953) and Benjamin (1959) in the context of other flow problems.

The limiting values of the wall stresses can be deduced by noting that $\bar{p} \to 2a$, $\mathrm{d}\bar{w}/\mathrm{d}y \to -a$, $\mathrm{d}\bar{u}/\mathrm{d}y \to -\alpha a$, when $\alpha \to \infty$.

The analysis of the temperature field is similar to the analysis of the flow field. We apply the transformations and obtain

$$\frac{\mathrm{d}\tilde{\Theta}}{\mathrm{d}y^2} + [-1 - \alpha^{-3}\tfrac{1}{2}Pr\,a y_1 + \alpha^{-4}\tfrac{1}{4}Pr\,y_1^2 + O(\alpha^{-6})]\,\tilde{\Theta} = \alpha^{-3}Pr\,a y_1\,\mathrm{e}^{-y_1} + O(\alpha^{-6}). \tag{4.44}$$

Following that, we assume $\bar{\Theta}$ in the form (4.37) and obtain a sequence of equations describing Θ_0, Θ_1, Θ_2, etc., which are easy to solve. These equations are listed in the Appendix. The complete solution in the case of an isothermal plate is

$$\bar{\Theta} = B\,\mathrm{e}^{-y_1} - \alpha^{-3}\tfrac{1}{4}Pr\,a y_1[1 + \tfrac{2}{3}B + (1 + \tfrac{1}{2}B)\,y_1]\,\mathrm{e}^{-y_1} + O(\alpha^{-4}), \tag{4.45}$$

where B is given by (3.12), and in the case of a constant-heat-flux plate is

$$\bar{\Theta} = -\alpha^{-3}\tfrac{1}{4}Pr\,a(1 + y_1 + y_1^2)\,\mathrm{e}^{-y_1} + O(\alpha^{-4}). \tag{4.46}$$

The limiting value of the increase of the heat flux for an isothermal plate can be deduced by noting that $\mathrm{d}\bar{\Theta}/\mathrm{d}y|_{y=0} \to -\alpha B$ when $\alpha \to \infty$, and the limiting value of the change of surface temperature of a plate with fixed heat flux can be deduced by noting that $\bar{\Theta}(0) \to 0$ when $\alpha \to \infty$.

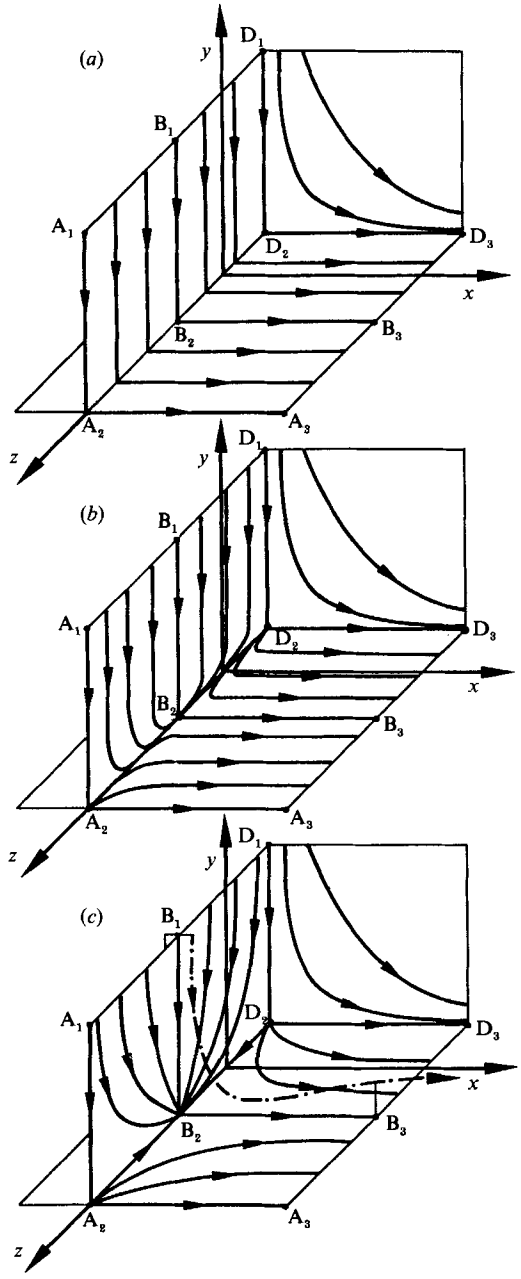

FIGURE 2. Topological structure of the stagnation flow over a plate with a wavy surface roughness. Cases (*a*) (flat plate), (*b*) and (*c*) correspond to progressively larger amplitude of the roughness.

5. Discussion

It is known that in a two-dimensional stagnation flow a degenerate stagnation line forms along which the skin friction is zero everywhere. The results of the present study show that arbitrary small three-dimensional perturbations in the shape of the leading edge cause a sequence of critical points (where the direction of the wall shear stress and the velocity field are not determined uniquely) to appear along such a

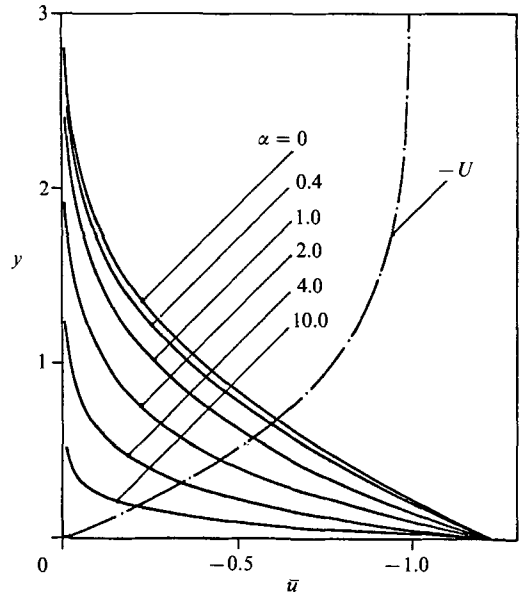

FIGURE 3. Variations of the amplitude of the x-velocity component $\bar{u}$ as a function of the wavenumber α.

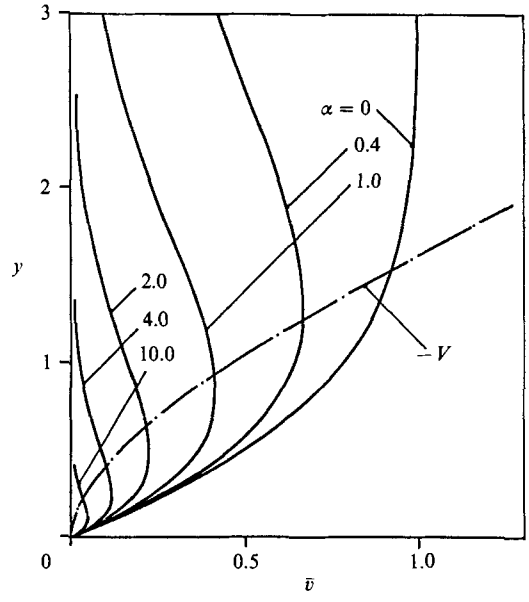

FIGURE 4. Variation of the amplitude of the y-velocity component $\bar{v}$ as a function of the wavenumber α.

stagnation line. The topology of the flow is shown in figure 2. The topology is very simple in the case of a flat plate (figure 2*a*). Small waviness of the surface produces the three-dimensional structure sketched in figure 2(*b*), where only one full period in the z-direction has been displayed. The critical points A_2 and D_2, which correspond to the 'peaks' of the roughness, exhibit a nodal point character in the (x, z)-plane and a saddle point character in the (y, z)-plane. In contrast, the critical point B_2, corresponding to the 'bottom' of the roughness, shows a saddle point character in the

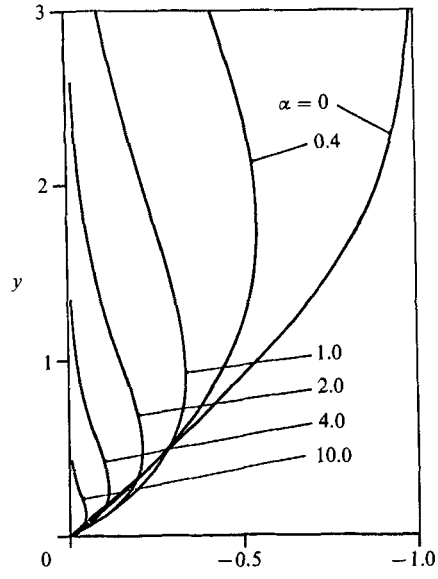

FIGURE 5. Variations of the amplitude of the z-velocity component $\bar{w}$ as a function of the wavenumber α.

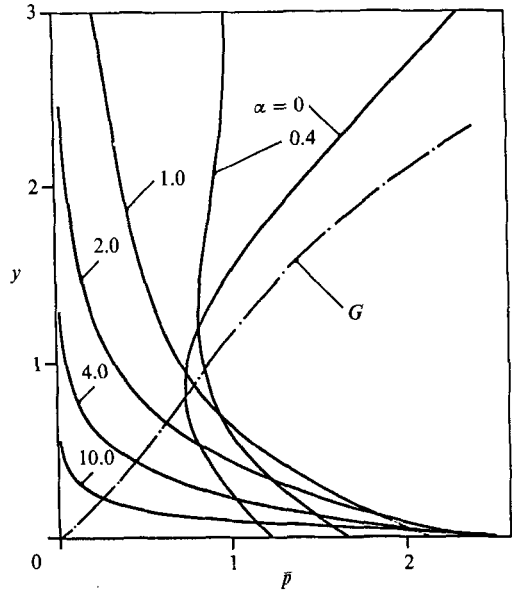

FIGURE 6. Variations of the amplitude of the pressure field $\bar{p}$ as a function of the wavenumber α.

(x, z)-plane and a nodal point character in the (y, z)-plane. The lines $A_1 A_2$, $B_2 B_3$ and $D_1 D_2$ become separatrices. An increase of the amplitude of the roughness leads to a more pronounced but qualitatively similar flow structure, as shown in figure 2(*c*). The flow does have a spanwise periodicity, but it does not develop into the form of counter-rotating vortex pairs. This can be seen in figures 3–7 displaying the velocity, pressure and vorticity fields. One should note that the $\bar{w}$-component (figure 5) does not have zeros in the interior of the flow. It is also interesting to note that since the

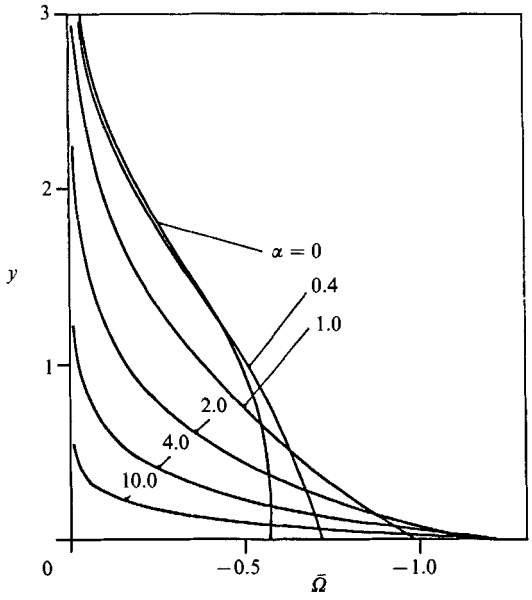

FIGURE 7. Variations of the amplitude of the x-component of vorticity $\bar{\Omega}$ as a function of the wavenumber α.

line B_2B_3 is a separatrix, one would expect a lift-off of the flow above this line due to conservation of mass.

Further increase of the amplitude of the roughness could result in a qualitative change in the topology of the flow and could lead, for example, to the generation of counter-rotating vortices. The character of the new topology cannot, however, be predicted by the linear theory described in this paper.

Flow disturbances are generated at the plate (figure 3) and are felt away from the plate, with the depth of this penetration being a strong function of the wavenumber α (figures 3–7). Here, disturbances generated by roughness of small wavenumber penetrate much further than disturbances generated by roughness of large wavenumber. The latter ones are limited to a very thin layer within which a simplified, i.e. linear, form of the undisturbed velocity profile is acceptable. The limits of validity of such a simplification have been assessed by carrying out the calculation with a linear velocity profile for $a \geqslant 1.0$ and by comparing results with those obtained with a complete velocity profile. It has been found that the error of surface quantities such as normal and shear stresses was not larger than 1 %.

The asymptotic form of the disturbance velocity field in the limit $\alpha \to 0$ which has been determined in §4.2 is displayed in figures 3–7. The results show that the $\bar{u}$ velocity component and the vorticity $\bar{\Omega}$ reach their asymptotic state very rapidly. These are the flow components that do not penetrate the region outside the flow boundary layer. The remaining flow components, i.e. $\bar{v}$, $\bar{w}$ and $\bar{p}$, are $O(1)$ outside the flow boundary layer and their evolution towards the asymptotic state with $\alpha \to 0$ is shown in figures 3–7. One should note that it is the long-wavelength waviness of the surface that is most difficult to eliminate in experiments (short-wavelength waviness can be eliminated by polishing). It is encouraging to know that the corresponding flow field already has a universal character for $\alpha < 0.1$, which corresponds to the magnitude of wavelength being of the order of the boundary-layer thickness. It can

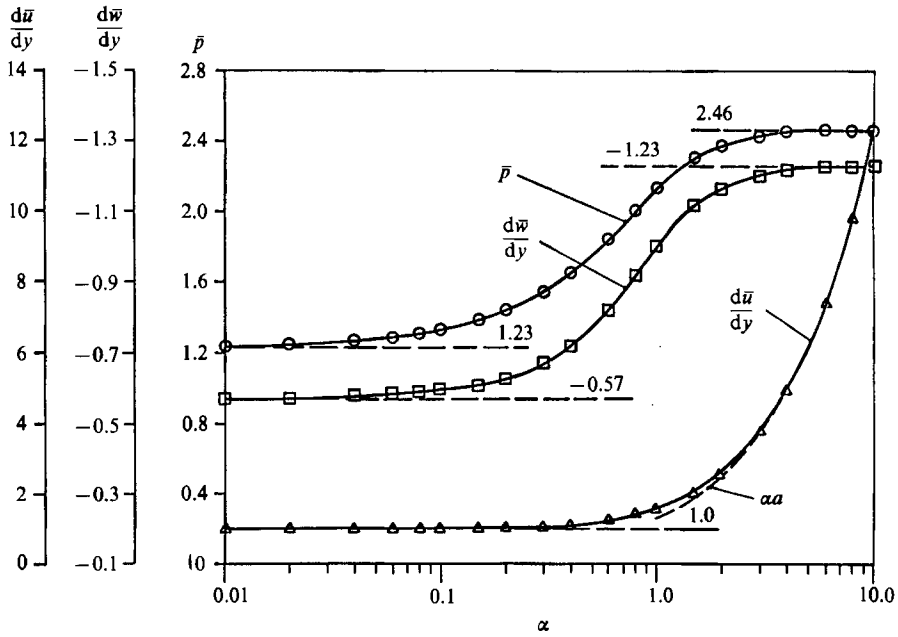

FIGURE 8. Variations of the surface values of $\bar{p}$, $d\bar{w}/dy$ and $d\bar{u}/dy$ as a function of the wavenumber α. Circles, squares and triangles denote computed points.

be concluded that the character of the flow, as described by (4.30) and displayed in figures 3–7, is most likely to be observed in experiments.

The character of the additional stress at the wall due to the presence of the surface roughness is described by (2.17). The calculated results do not exhibit any unexpected phenomena. They show an increase of shear acting on the 'peaks' of the roughness in the x-direction and an analogous decrease in the shear acting on the 'valleys'. There is an additional shear acting in the spanwise direction, and it acts from the peak towards the valley position. The net effect of shear is such that it would tend to eliminate the roughness in the case of erosion. The additional normal stress pushes the peaks downwards and it would tend to eliminate them if the plate were flexible. Variations of the wall stresses as a function of the wavenumber α can be deduced from the results shown in figure 8. The appropriate limits for $\alpha \to 0$ and $\alpha \to \infty$ have been given explicitly in §4.2 and §4.3, respectively. We note a rapid disappearance of $\Delta\sigma_{yy}$ and $\Delta\sigma_{yx}$ and equally rapid emergence of an asymptotic form of $\Delta\sigma_{yx}$ for $\alpha \to 0$. We also note the existence of the absolute upper limits for $\Delta\sigma_{yy}$ and $\Delta\sigma_{yz}$, which are reached for $\alpha \to \infty$, and an unbounded (proportional to α) growth of $\Delta\sigma_{yx}$ with $\alpha \to \infty$. The last result suggests that the flow would be more effective in eliminating short- rather than long-wavelength roughness through friction if erosion or ablation were admitted.

The effects of roughness on heat transfer in the case of an isothermal plate are illustrated in figures 9–11 for two typical cases of Prandtl number, $Pr = 0.71$ (air) and $Pr = 7.0$ (water). It is seen that the disturbances are limited to the interior of the thermal boundary layer. We note a rapid approach of the character of the temperature field towards a universal form given by (4.32) with $\alpha \to 0$, the approach being more rapid for a fluid of large Prandtl number. The large wavenumber approximation provides a much better approximation in the case of a fluid of small

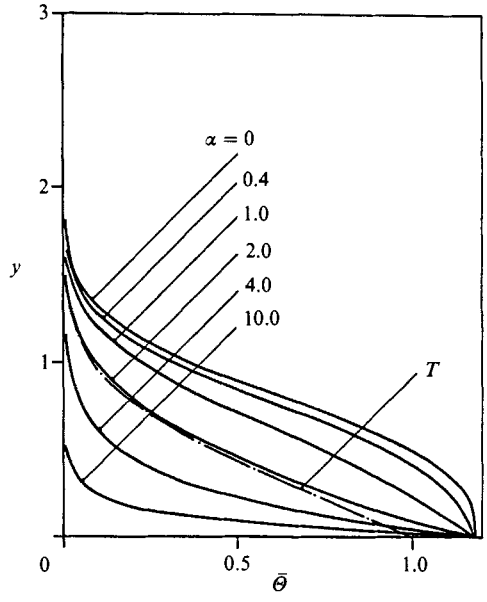

FIGURE 9. Variations of the amplitude of the temperature $\bar{\Theta}$ as a function of the wavenumber α for $Pr = 0.71$ and an isothermal plate.

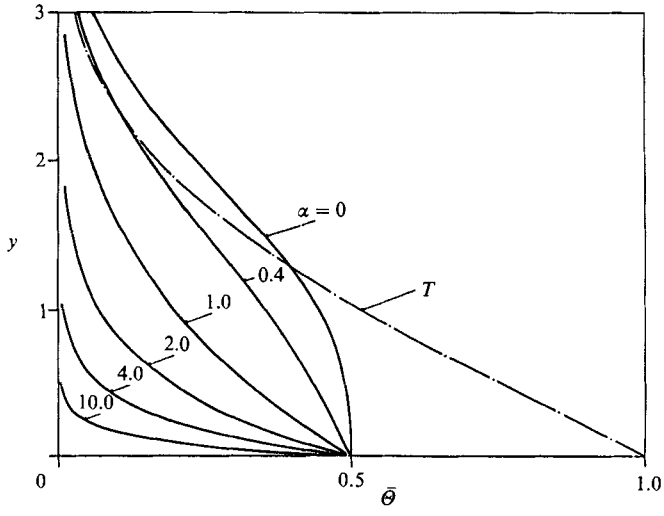

FIGURE 10. Variations of the amplitude of the temperature $\bar{\Theta}$ as a function of the wavenumber α for $Pr = 7.0$ and an isothermal plate.

Prandtl number, which is to be expected. The modification of the heat flow at the surface of the plate is given by (2.18). The calculated results show that there is an increase of heat flow from the plate to the fluid around the peaks of the roughness and a corresponding rise in the temperature of the fluid above the peaks when the plate is being cooled by the fluid. The situation is similar in the case of a plate heated by the fluid except that the signs are reversed, i.e. there is an increase of heat flow into the wall at the peak. Thus, in all cases there is an increase of heat transport through the peak area, which is to be expected. Figure 11 shows that Δq_n increases

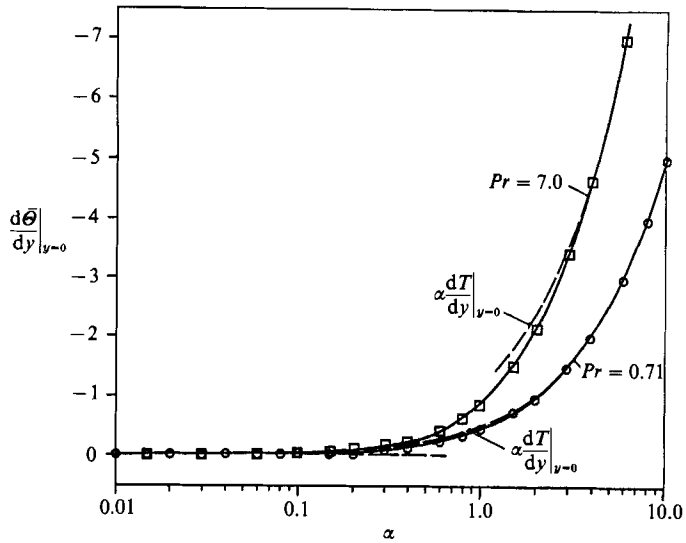

FIGURE 11. Variations of the surface value of $d\bar{\Theta}/dy$ as a function of the wavenumber α. Circles and squares denote computed points.

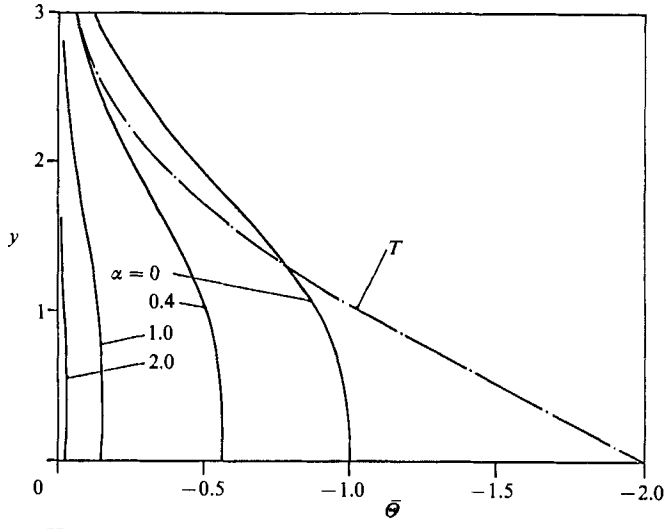

FIGURE 12. Variations of the amplitude of the temperature $\bar{\Theta}$ as a function of the wavenumber α for $Pr = 0.71$ and a constant-heat-flux plate.

with an increase of the Prandtl number and that it is a strong function of the wavenumber α, being negligible for small wavenumbers ($\lim d\bar{\Theta}/dy|_{y=0} = 0$ as $\alpha \to 0$) and its amplitude growing proportionally to α for large wavenumbers ($\lim d\bar{\Theta}/dy|_{y=0} = \alpha\, dT/dy|_{y=0}$ as $\alpha \to \infty$). We note that the asymptotic solutions provide a good approximation of the surface heat flux over the whole range of variations of α, with the error increasing with an increase of the Prandtl number.

The effects of roughness on heat transfer in the case of a plate with a constant heat flux are illustrated in figures 12–14 for the same values of Prandtl number. The qualitative behaviour of the disturbance field is similar to the previous case, i.e. the disturbances are limited to the interior of the thermal boundary layer; there is a

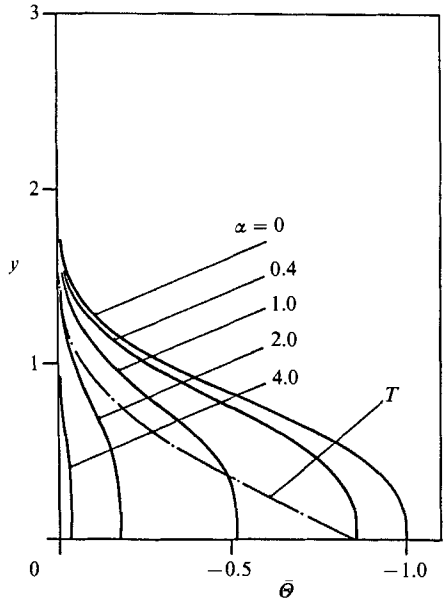

FIGURE 13. Variations of the amplitude of the temperature $\bar{\Theta}$ as a function of the wavenumber α for $Pr = 7.0$ and a constant-heat-flux plate.

rapid approach of the temperature field towards an asymptotic form with $\alpha \to 0$; this approach is more rapid for fluids of a large Prandtl number; and the large-wavenumber approximation is better in the case of small-Prandtl-number fluids. The modification of the wall temperature is given by (2.19). The calculated results show an increase of the wall temperature in the peak area and a decrease of fluid temperature above the peak in the case of heat flowing into the wall. When the heat flow changes direction, the peak becomes colder and the fluid above it becomes hotter. Thus the peak areas of a heated plate and the valley areas of a cooled plate can be subjected to overheating. Figure 14 shows that ΔT_w increases with a decrease of the Prandtl number and that it is a strong function of the wavenumber α, being negligible for small wavenumbers ($\lim \bar{\Theta}(0) = -1$ as $\alpha \to 0$) and its amplitude approaching unity for large wavenumbers ($\lim \bar{\Theta}(0) = 0$ as $\alpha \to \infty$).

Surface roughness could be responsible for permanent damage to the surface of the plate. The possible mechanism involves generation of thermal stresses due to redistribution of heat flow into the peaks of the roughness, as discussed above. In the limit $\alpha \to \infty$, thermal gradients increase at a rate no less than $O(\alpha)$ and could become large enough to cause surface cracking.

In order to compare sensitivity of the wall shear stress and heat transport to the presence of surface roughness, relative changes of σ_{yx} [$e_1 = \epsilon\alpha^{-1}(\mathrm{d}\bar{u}/\mathrm{d}y|_{y=0} - 1)\sin(\alpha z)$], heat flux through an isothermal plate [$e_2 = \epsilon(\mathrm{d}\bar{\Theta}/\mathrm{d}y|_{y=0}/(\mathrm{d}T/\mathrm{d}y|_{y=0}))\sin(\alpha z)$] and temperature of a plate with a constant heat flux [$e_3 = \epsilon(1+\bar{\Theta}(0))/T(0)\sin(\alpha z)$] were evaluated. The numerical values for $\alpha = 1.0$ are $e_1 = 0.44\epsilon\sin z$, $e_2 = 0.91\epsilon\sin z$, $0.72A\epsilon\sin z$ and $e_3 = -0.43\epsilon\sin z$, $-0.59\epsilon\sin z$ for $Pr = 0.71$, 7.0 respectively, and show a somewhat higher sensitivity of heat transport compared to the sensitivity of the shear stress to the presence of roughness. This sensitivity decreases with an increase of Prandtl number in the case of an isothermal plate and increases in the case of a constant heat flux plate.

The results discussed above provide a complete and detailed picture of the

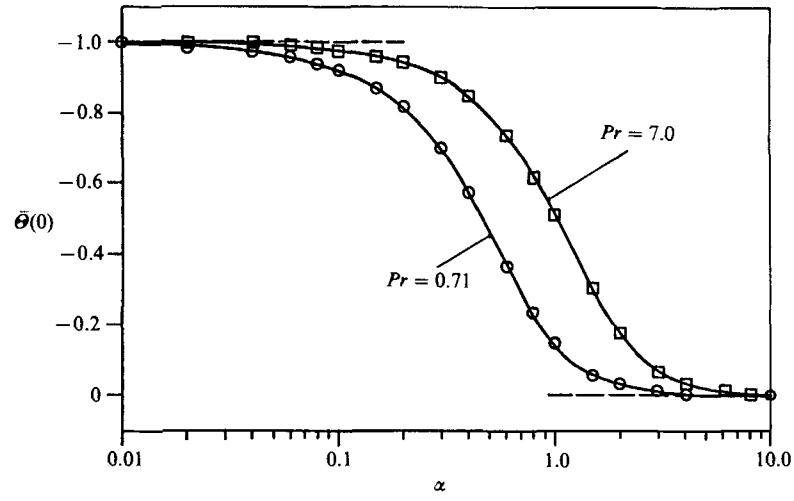

FIGURE 14. Variations of surface value of $\bar{\theta}$ as a function of the wavenumber α. Circles and squares denote computed points.

structure of the flow and the temperature fields associated with surface roughness. An interesting question arises regarding the stability of such a flow and this question could be addressed on its own merits. Here, we would like to point out a possible role which surface roughness could play in the instability of the stagnation flow. It is well known that three-dimensional longitudinal (i.e. aligned in the x-direction) vortex pairs can be observed in the stagnation regions of cylinders (Morkovin 1979). It is also known that while stagnation flows are linearly stable (Wilson & Gladwell 1978), the secondary flows could be generated by the so-called vorticity amplification mechanism (Sutera *et al.* 1963; Sutera 1965; Sadeh, Sutera & Maeder 1970), which requires the presence of a certain type of disturbance in the oncoming flow. The presence of a vorticity-amplification-type mechanism has been confirmed by recent experiments (Kottke 1986; Böttcher 1987) showing that the vortex structures could be found in the stagnation region only if disturbances produced by screens were present in the oncoming flow. The spacing of the vortex pairs was found to be equal to that of the jets in the wake of the screens. Thus, the flow in the stagnation region was merely an image of the flow downstream of the screen. Surface roughness provides an alternative way of introducing disturbances into the flow and it is postulated here that these disturbances could grow and lead to the appearance of a secondary flow without the presence of external disturbances in the oncoming flow. It has been shown in §4.2 that surface roughness influences the flow far upstream if the wavenumber α is sufficiently small. The surface-roughness-generated disturbances could then trigger an amplification process, where the initial stages of the spatial amplification outside the boundary layer would be governed by the solution proportional to constant b_4 in (4.4). Here the only condition for existence of the spatial amplification would be $\alpha < 1$, as discussed in §4.1. This condition is similar to the one found in the vorticity amplification theory (Sutera *et al.* 1963). It should be noted that while the process postulated above is likely, its existence requires an experimental verification.

Surface roughness acts as a source of steady streamwise vorticity, as shown in figure 7. Such vorticity is one of the possible ways of forcing boundary-layer instability (Morkovin 1988; Herbert 1988). It has been demonstrated by Wilkinson

& Malik (1985) that in the case of rotating disk flow the well-known growing spiral vortices were driven by surface roughness. The leading-edge roughness analysed here could provide a similar path for the receptivity problem.

The first author wishes to acknowledge the financial sponsorship of the Alexander von Humboldt Foundation of the Federal Republic of Germany and the Natural Sciences and Engineering Research Council of Canada.

Appendix

Equations describing disturbance velocity and pressure fields in the limit $\alpha \to \infty$.

Order α^{-1}:

$$\hat{L}_1(u_1, v_1, w_1, p_1) = 0, \quad \hat{L}_2(u_1, v_1, w_1, p_1) = 0, \tag{A 1a, b}$$

$$\hat{L}_3(u_1, v_1, w_1, p_1) = 0, \quad \hat{L}_4(u_1, v_1, w_1, p_1) = -u_0, \tag{A 1c, d}$$

$$u_1 = v_1 = w_1 = 0 \quad \text{at} \quad y_1 = 0, \qquad u_1 \to 0, \quad v_1 \to 0, \quad w_1 \to 0 \quad \text{as} \quad y_1 \to \infty. \tag{A 1e, f}$$

Order α^{-2}:

$$\hat{L}_1(u_2, v_2, w_2, p_2) = av_0, \quad \hat{L}_2(u_2, v_2, w_2, p_2) = 0, \tag{A 2a, b}$$

$$\hat{L}_3(u_2, v_2, w_2, p_2) = 0, \quad \hat{L}_4(u_2, v_2, w_2, p_2) = -u_1, \tag{A 2c, d}$$

$$u_2 = v_2 = w_2 = 0 \quad \text{at} \quad y_1 = 0, \qquad u_2 \to 0, \quad v_2 \to 0, \quad w_2 \to 0 \quad \text{as} \quad y_1 \to \infty. \tag{A 2e, f}$$

Order α^{-3}:

$$\hat{L}_1(u_3, v_3, w_3, p_3) = av_1 - v_0 y_1 + \tfrac{5}{2} a y_1 u_0, \tag{A 3a}$$

$$\hat{L}_2(u_3, v_3, w_3, p_3) = -\tfrac{1}{4} a y_1^2 \hat{p}_0 - \tfrac{1}{2} a y_1 v_0, \tag{A 3b}$$

$$\hat{L}_3(u_3, v_3, w_3, p_3) = \tfrac{1}{2} a y_1 w_0, \quad \hat{L}_4(u_3, v_3, w_3, p_3) = \tfrac{1}{4} a y_1^2 v_0, \tag{A 3c, d}$$

$$u_3 = v_3 = w_3 = 0 \quad \text{at} \quad y_1 = 0, \qquad u_3 \to 0, \quad v_3 \to 0, \quad w_3 \to 0 \quad \text{as} \quad y_1 \to \infty. \tag{A 3e, f}$$

Order α^{-4}:

$$\hat{L}_1(u_4, v_4, w_4, p_4) = av_2 - y_1 v_1 + \tfrac{5}{2} a y_1 u_1 - \tfrac{5}{4} y_1^2 u_0, \tag{A 4a}$$

$$\hat{L}_2(u_4, v_4, w_4, p_4) = -\tfrac{1}{4} a y_1^2 \hat{p}_1 + \tfrac{1}{12} y_1^3 \hat{p}_0 - \tfrac{1}{2} a y_1 v_1 + \tfrac{1}{4} y_1^2 v_0, \tag{A 4b}$$

$$\hat{L}_3(u_4, v_4, w_4, p_4) = \tfrac{1}{2} a y_1 w_1 - \tfrac{1}{4} y_1^2 w_0, \tag{A 4c}$$

$$\hat{L}_4(u_4, v_4, w_4, p_4) = \tfrac{1}{4} a y_1^2 v_1 - \tfrac{1}{12} y_1^3 v_0, \tag{A 4d}$$

$$u_4 = v_4 = w_4 = 0 \quad \text{at} \quad y_1 = 0, \qquad u_4 \to 0, \quad v_4 \to 0, \quad w_4 \to 0 \quad \text{as} \quad y_1 \to \infty. \tag{A 4e, f}$$

Higher-order equations could be written in a similar way. We note that the basic flow effects only appear in the equations $O(\alpha^2)$ and higher.

Equations describing disturbance temperature field.

Order α^0:

$$\frac{\mathrm{d}^2 \Theta_0}{\mathrm{d}y_1^2} - \Theta_0 = 0, \quad \Theta_0 = B \quad \text{or} \quad \frac{\mathrm{d}\Theta_0}{\mathrm{d}y_1} = 0 \quad \text{at} \quad y_1 = 0, \qquad \Theta_0 \to 0 \quad \text{as} \quad y_1 \to \infty. \tag{A 5a–c}$$

Order α^{-1}:

$$\frac{\mathrm{d}^2\Theta_1}{\mathrm{d}y_1^2}-\Theta_1=0, \quad \Theta_1=0 \quad \text{or} \quad \frac{\mathrm{d}\Theta_1}{\mathrm{d}y}=0 \quad \text{at} \quad y_1=0, \qquad \Theta_1\to 0 \quad \text{as} \quad y_1\to\infty. \tag{A 6a–c}$$

Order α^{-2}:

$$\frac{\mathrm{d}^2\Theta_2}{\mathrm{d}y_1^2}-\Theta_2=0, \quad \Theta_2=0 \quad \text{or} \quad \frac{\mathrm{d}\Theta_2}{\mathrm{d}y_1}=0 \quad \text{at} \quad y_1=0, \qquad \Theta_2\to 0 \quad \text{as} \quad y_1\to\infty. \tag{A 7a–c}$$

Order α^{-3}:

$$\frac{\mathrm{d}^2\Theta_3}{\mathrm{d}y_1^2}-\Theta_3=\tfrac{1}{2}Pr\,a y_1\Theta_0+Pr\,a y_1\,\mathrm{e}^{-y_1}, \tag{A 8a}$$

$$\Theta_3=0 \quad \text{or} \quad \frac{\mathrm{d}\Theta_3}{\mathrm{d}y_1}=0 \quad \text{at} \quad y_1=0, \qquad \Theta_3\to 0 \quad \text{as} \quad y_1\to\infty. \tag{A 8b, c}$$

Order α^{-4}:

$$\frac{\mathrm{d}^2\Theta_4}{\mathrm{d}y_1^2}-\Theta_4=\tfrac{1}{2}Pr\,a y_1\Theta_1-\tfrac{1}{4}Pr\,a y_1^2\Theta_0, \tag{A 9a}$$

$$\Theta_4=0 \quad \text{or} \quad \frac{\mathrm{d}\Theta_4}{\mathrm{d}y_1}=0 \quad \text{at} \quad y_1=0, \qquad \Theta_4\to 0 \quad \text{as} \quad y_1\to\infty. \tag{A 9b, c}$$

Higher-order equations could be written in a similar way.

REFERENCES

Abramowitz, M. & Stegun, I. A. 1965 *Handbook of Mathematical Functions*. Dover.

Benjamin, T. B. 1959 Shearing flow over a wavy boundary. *J. Fluid Mech.* **6**, 161.

Böttcher, J. 1987 The flow downstream of screens and its influence on the flow in the stagnation region. *AIAA Paper* 87-1258, presented at the *AIAA 19th Fluid Dynamics, Plasma Dynamics and Lasers Conf., Honolulu, USA*.

Fisher, T. M. & Dallmann, U. 1987 Theoretical investigation of secondary instability of three-dimensional boundary-layer flows. *AIAA Paper* 87-1338, presented at the *AIAA 19th Fluid Dynamics, Plasma Dynamics and Lasers Conf., Honolulu, USA*.

Floryan, J. M. & Saric, W. S. 1984 Wavelength selection and growth of Görtler vortices. *AIAA J.* **22**, 1529.

Goldstein, M. E. 1983 The evolution of Tollmien–Schlichting waves near a leading edge. *J. Fluid Mech.* **127**, 59.

Goldstein, S. 1938 *Modern Developments in Fluid Mechanics*. Clarendon.

Görtler, H. 1955 Dreidimensionale Instabilität der ebenen Staupunktströmung gegenüber wirbelartigen Storungen. In *Fifty Years of Boundary Layer Research* (ed. H. Görtler & W. Tollmien), p. 304. Braunschweig: Vieweg und Sohn.

Hämmerlin, G. 1955 Zur Instabilitätstheorie der ebenen Staupunkströmung. In *Fifty Years of Boundary Layer Research* (ed. H. Görtler & W. Tollmien), p. 315. Braunschweig: Vieweg und Sohn.

Herbert, T. 1988 Secondary instability of boundary layers. *Ann. Rev. Fluid Mech.* **20**, 487.

Kestin, J. 1966 The effect of free-stream turbulence on heat transfer rates. *Adv. Heat Transfer* **3**, 1.

Kottke, V. 1986 On the visualization of longitudinal vortices in stagnation flow. In *Flow Visualization IV, Proc. Fourth Intl Symp. on Flow Visualization* (ed. C. Véret), pp. 321–326. Hemisphere.

Lighthill, M. J. 1953 On boundary layers and upstream influence II. Supersonic flows without separation. *Proc. R. Soc. Lond.* A **217**, 478.

LYELL, M. J. & HUERRE, P. 1985 Linear and nonlinear stability of plane stagnation flow. *J. Fluid Mech.* **161**, 295.

MORGAN, V. T. 1973 The heat transfer from bare stranded conductors by natural and forced convection in air. *Intl J. Heat Mass Transfer* **16**, 2023.

MORKOVIN, M. V. 1979 On the question of instabilities upstream of cylindrical bodies. *NASA Contractor Rep.* 3231.

MORKOVIN, M. V. 1988 Recent insights into stability and transition to turbulence in open flow system. *NASA Contractor Rep* 181693.

NAYFEH, A. H. 1973 *Perturbation Methods.* Wiley & Sons.

NAYFEH, A. H. 1981 Effects of streamwise vortices on Tollmien–Schlichting waves. *J. Fluid Mech.* **107**, 441.

NITSCHKE-KOWSKY, P. 1986 Experimentelle Untersuchungen zu Stabilität und Umschlag dreidimensionaler Grenzschichten. Dissertatin zum Doktor rer.nat., Georg-August-Universität, Göttingen, FRG.

NITSCHKE-KOWSKY, P. & BIPPES, H. 1988 Instability and transition of a three-dimensional boundary layer over a swept flat plate. *Phys. Fluids* **31**, 786.

PEREYRA, V. 1979 PASVA 3: An adaptive finite-difference Fortran program for first order nonlinear boundary value problems. In *Codes for Boundary-Value Problems in Ordinary Differential Equations.* Lecture Notes in Computer Science, vol. 76, p. 67. Springer.

PFENNIGER, W. 1977 Laminar flow control laminarization. *AGARD Rep.* 654, 3-1.

POLL, D. I. A. 1979 Transition in the infinite swept attachment line boundary layer. *Aeronaut. Q.* **30**, 607.

RESHOTKO, E. 1976 Boundary-layer stability and transition. *Ann. Rev. Fluid Mech.* **8**, 311.

SADEH, W. Z., SUTERA, S. P. & MAEDER, P. F. 1970 Analysis of vorticity amplification in the flow approaching a two-dimensional stagnation point. *Z. Angew. Math. Phys.* **21**, 699.

SPALART, P. R. 1989 Direct numerical study of leading edge contamination. *AGARD*-CP-438, *Paper no.* 5.

SRIVASTAVA, K. M. & DALLMANN, U. 1987 Effect of streamwise vortices on Tollmien–Schlichting waves in growing boundary layers. *Phys. Fluids* **30**, 1005.

SUTERA, S. P. 1965 Vorticity amplification in stagnation point flow and its effect on heat transfer. *J. Fluid Mech.* **21**, 513.

SUTERA, S. P., MEADER, P. F. & KESTIN, J. 1963 On the sensitivity of heat transfer in the stagnation-point boundary layer to free-stream vorticity. *J. Fluid Mech.* **16**, 497.

WILKINSON, S. P. & MALIK, E. C. 1985 Stability experiments in the flow over a rotating disk. *AIAA J.* **23**, 588.

WILSON, S. & GLADWELL, I. 1978 The stability of a two-dimensional stagnation flow to three-dimensional disturbances. *J. Fluid Mech.* **84**, 517.